

On certain properties of the compact Zakharov equation

Francesco Fedele[†]

Address: School of Civil and Environmental Engineering,
School of Electrical and Computer Engineering,
Georgia Institute of Technology, Atlanta, Georgia, USA

(Received ?; revised ?; accepted ?. - To be entered by editorial office)

Long-time evolution of a weakly perturbed wavetrain near the modulational instability threshold is examined within the framework of the compact Zakharov equation for unidirectional deep-water waves (Dyachenko & Zakharov (2011)). Multiple-scale solutions reveal that a perturbation to a slightly unstable uniform wavetrain of steepness μ slowly evolves according to a nonlinear Schrodinger equation. In particular, for small carrier wave steepness $\mu < \mu_1 \approx 0.27$ the perturbation dynamics is of focusing type and the long-time behavior is characterized by the Fermi-Pasta-Ulam recurrence, the signature of breather interactions. However, the amplitude of breathers and their likelihood of occurrence tend to diminish as μ increases while the Benjamin-Feir index decreases and becomes nil at μ_1 . This indicates that homoclinic orbits persist only for small values of wave steepness $\mu \ll \mu_1$, in agreement with recent experimental and numerical observations of breathers.

When the compact Zakharov equation is beyond its nominal range of validity, i.e. for $\mu > \mu_1$, predictions seem to foreshadow a dynamical trend to wave breaking. In particular, the perturbation dynamics becomes of defocusing type, and nonlinearities tend to stabilize a linearly unstable wavetrain as the Fermi-Pasta-Ulam recurrence is suppressed. At $\mu = \mu_c \approx 0.577$, subharmonic perturbations restabilize and superharmonic instability appears, possibly indicating that wave dynamical behavior changes at large steepness, in qualitative agreement with the numerical simulations of Longuet-Higgins & Cokelet (1978) for steep waves. Indeed, for $\mu > \mu_c$ a multiple-scale perturbation analysis reveals that a weak narrowband perturbation to a uniform wavetrain evolves in accord with a modified Korteweg-de Vries/Camassa-Holm type equation, again implying a possible mechanism conducive to wave breaking.

Key words: Breathers, Hamiltonian, modulational instability, multiple-scale perturbation, nonlinear waves, recurrence, wave breaking.

1. Introduction

Unidirectional weakly nonlinear narrowband wavetrains evolve in deep water according to the nonlinear Schrodinger (NLS) equation, which is integrable. The associated Lax-pairs were discovered by Zakharov & Shabat (1972), who unveiled the dynamics of solitons via the Inverse Scattering Transform (IST) (see e.g. Ablowitz & Segur (1981)). Another important asymptotic model of the Euler equations for the free-surface of an ideal flow is the Zakharov (Z) integro-differential equation, which is not integrable (Zakharov

[†] Email address for correspondence: E-mail address: fedele@gatech.edu

(1999) and Dyachenko & Zakharov (2013)). The Z equation is derived by means of a third order expansion of the Hamiltonian in wave steepness, where fast non-resonant interactions are eliminated via a canonical transformation that preserves the Hamiltonian structure (Krasitskii (1994)). The equation is valid for weakly nonlinear four-wave interactions, but it has no constraints on the spectral bandwidth. For unidirectional waves with narrowband spectra it reduces to the NLS or the higher order Dysthe (1979) equation.

It is well known that a finite-amplitude uniform wavetrain is unstable to infinitesimal subharmonic perturbations, the so-called modulational instability (MI) or Benjamin-Feir instability (Benjamin & Feir (1967); Benjamin (1967)). Whereas the MI growth rate implied by the NLS model tends to overestimate experimental data, growth rates predicted from the Z equation are lower and comparable to the values observed in experiments (Crawford *et al.* (1981); Janssen (1983)). Further, Janssen (1981) showed within the NLS framework that in the absence of viscous dissipation, a linearly unstable wavetrain does not evolve to a steady state, but the long-time behavior is characterized by successive modulation and demodulation cycles, viz. the Fermi-Pasta-Ulam (FPU) recurrence (Fermi (1955)). This is the signature of breathers, homoclinic orbits to an unstable uniform wavetrain (Peregrine (1983) and Osborne (2010), see also Henderson *et al.* (1999) and Tanaka (1990)).

NLS breathers have been the subject of numerous studies, in particular, to explain rogue wave formation (Dysthe & Trulsen (1999); Osborne *et al.* (2000); Peregrine (1983); Kharif *et al.* (2009); Kharif & Pelinovsky (2003); Janssen (2003); Gramstad & Trulsen (2007); Dysthe & Muller (2008); Clamond *et al.* (2006)). Recently, Chabchoub *et al.* (2011) and Chabchoub *et al.* (2012) provided laboratory observations of higher-order breathers at sufficiently small values of wave steepness ($\sim 0.01 - 0.09$), confirmed by numerical simulations (Slunyaev *et al.* (2013)).

The experimental and numerical results describing the nature of breathers as briefly reviewed in the preceding provide the principal motivation for this study. In particular, we aim to investigate further the modulational properties of the Z equation for unidirectional deep-water waves. This should provide new insight into the occurrence of breathers as observed in the experimental studies aforementioned. To achieve this objective, we shall study the weakly nonlinear space-time evolution of a unstable uniform wavetrain of the compact Z equation, hereafter referred to as cDZ. The compact form follows from a canonical transformation of the Z equation and eliminates trivial resonant quartet interactions (Dyachenko & Zakharov (2011)). As a result, the Z model reduces to a generalized derivative NLS type equation (Fedele & Dutykh (2012)).

The long-time behavior near the MI threshold is determined by means of multiple-scale perturbation techniques (see e.g. Yang (2010)). Although the cDZ equation is strictly valid for weakly nonlinear four-wave interactions, it captures new features that indicate finite-time blowup or wave breaking, not modeled by the one-dimensional (1D) NLS nor the higher-order Dysthe (1979) equation. Therefore we shall also explore its properties for relatively large steepness values beyond the range of validity since the resulting predictions may serve to indicate the behavior of waves as they steepen and approach breaking.

The remainder of the paper is organized as follows. In section 2, the cDZ equation is introduced, and then the associated equations in terms of local wave amplitude and phase are derived. The linear instability of a uniform wavetrain is presented in section 3 and followed by a multiple-scale perturbation analysis to study the long-time dynamics of a weakly perturbed wavetrain in section 4. This is followed by a discussion of the theoretical results and concluding remarks.

2. Compact Zakharov equation

Following Fedele & Dutykh (2012), we introduce a reference frame moving at the group velocity $c_g = \omega_0/(2k_0)$ in deep water and the dimensionless scales $X = k_0(x - c_g t)$ and $T = \omega_0 t$, with $k_0 = \omega_0^2/g$ and ω_0 as the wavenumber and frequency of the carrier wave $e^{i(k_0 x - \omega_0 t)}$. The leading order wave surface η is given by

$$k_0 \eta(X, T) = B(X, T) e^{i(k_0 x - \omega_0 t)} + \text{c.c.}, \quad (2.1)$$

and non-dimensional envelope B follows from

$$i \partial_T B = \frac{\delta \mathcal{H}}{\delta B^*}, \quad (2.2)$$

where δ denotes variational differentiation,

$$\mathcal{H} = \int_{\mathbb{R}} \left[B^* \Omega B + \frac{i}{4} |SB|^2 [B(SB)^* - B^* SB] - \frac{1}{2} |SB|^2 \mathbf{H}(\partial_X |B|^2) \right] dX \quad (2.3)$$

is the Hamiltonian and

$$\mathcal{S} = \partial_X + i, \quad \Omega = \frac{1}{8} \partial_X X,$$

with $\mathbf{H}(g)$ being the Hilbert transform of $g(X)$. The preceding do not include third- and higher-order corrections to dispersion to simplify the analysis of the cDZ. Further, higher-order non-resonant corrections to (2.2) hidden within the full canonical transformation of Dyachenko & Zakharov (2011) are not accounted for, and the carrier wave steepness is defined as

$$\mu = k_0 a_0 = 2 |B|, \quad (2.4)$$

where $a_0 = 2 |B|/k_0$ is the amplitude of η . Also note that (2.2) is valid if all the Fourier components comprising the spectrum of η travel in the same direction (Dyachenko & Zakharov (2011)). This condition is satisfied if $k_0 \gg 1$ or the spectrum of B has negligible energy for wavenumbers $k < -k_0$, viz. the spectral bandwidth $\Delta k/k_0$ is less than unity. Otherwise, a projection operator P^+ would have to be applied to the nonlinear term of (2.2) to nullify Fourier modes with wavenumbers $k < -k_0$. We assume that the conditions for excluding P^+ are satisfied in the present analysis.

The uniform wavetrain solution of the cDZ equation is

$$B_0(T) = \sqrt{E_0} e^{-i E_0 T}, \quad (2.5)$$

where E_0 is the squared amplitude of the wavetrain.

The stability of B_0 to infinitesimal perturbations and its weakly nonlinear evolution over the long-time scale can be studied by considering the local form of the cDZ equation, ignoring the effects of wave-induced currents. This does not affect the eventual conclusions of the present analysis. Under this setting, define

$$B = \sqrt{E(X, T)} e^{i \phi(X, T) - i E_0 T}, \quad (2.6)$$

with E as the squared envelope amplitude and ϕ the associated phase. By neglecting non-local terms in (2.3), the Lagrangian \mathcal{L} associated with (2.2), namely

$$\mathcal{L} = \frac{i}{2} (B^* \partial_T B - \partial_T B^* B) - \mathcal{H} \quad (2.7)$$

reduces to

$$\mathcal{L} = -E(E_0 + \phi_T) - \frac{4E^2(-\phi_X^2 + 4E(1 + \phi_X)^3) + E_X^2(-1 + 4E(1 + \phi_X))}{32E}, \quad (2.8)$$

where subscripts denote partial derivatives with respect to T or X . Minimizing the action via variational differentiation of \mathcal{L} yields the dynamical equations for E and ϕ as

$$\begin{cases} \partial_T \phi + \omega = 0 \\ \partial_T E + \partial_X (VE) = 0 \end{cases}, \quad (2.9)$$

where, in the reference frame X moving at the group speed c_g , the local frequency of the wavetrain is given by

$$\begin{aligned} \omega &= \frac{\partial \mathcal{H}}{\partial E} - \partial_X \left(\frac{\partial \mathcal{H}}{\partial E_X} \right) = \frac{E_{XX}}{16E} [1 - 4E(1 + \phi_X)] + \\ &\quad - \frac{1}{32} \left(\frac{E_X}{E} \right)^2 - \frac{\phi_X^2}{8} + E(1 + \phi_X)^3 - E_0 - \frac{1}{4} E_X \phi_X, \end{aligned} \quad (2.10)$$

and the energy flux velocity by

$$V = \frac{1}{E} \frac{\partial \mathcal{H}}{\partial \phi_X} = -\frac{\phi_X}{4} (1 - 12E) + \frac{3}{2} E + \frac{1}{8} \left[\frac{E_X^2}{E} + 12E\phi_X^2 \right]. \quad (2.11)$$

Note that if the cubic terms are neglected, (2.9) reduces to the NLS model (Janssen (1981) and Chu & Mei (1970)).

Next, we can exploit the conservative nature of the system described by (2.9), formulated in terms of E and the local wavenumber $K = \phi_X$. In particular, the differentiation of the first equation in (2.9) leads to

$$\begin{cases} \partial_T K + \partial_X \omega = 0 \\ \partial_T E + \partial_X (VE) = 0 \end{cases}. \quad (2.12)$$

Here, E and K can be interpreted as the 'density' and 'momentum' of a gas with 'pressure' ω . Moreover, their space averages are invariants of motion.

3. Linear stability of a uniform wavetrain

In accord with the ansatz (2.6) and (2.9), the uniform wavetrain solution (2.5) is given in terms of E and ϕ as

$$\mathbf{v}_0 = \begin{bmatrix} E_0 \\ 0 \end{bmatrix}. \quad (3.1)$$

To proceed with the linear stability analysis of \mathbf{v}_0 , we perturb it as

$$\mathbf{v} = \mathbf{v}_0 + \epsilon \mathbf{v}_1, \quad (3.2)$$

where

$$\mathbf{v}_1 = \begin{bmatrix} E_1(X, T) \\ \phi_1(X, T) \end{bmatrix},$$

and ϵ is a small parameter. Linearizing (2.9) yields the vector equation

$$\partial_T \mathbf{v}_1 + \mathcal{M}_0 \mathbf{v}_1 = 0 \quad (3.3)$$

where

$$\mathbf{v}_1 = \begin{bmatrix} E_1 \\ \phi_1 \end{bmatrix}, \quad \mathcal{M}_0 = \begin{bmatrix} 3E_0 \partial_X & \frac{-E_0(1-12E_0)}{4} \partial_{XX} \\ 1 + \frac{1-4E_0}{16E_0} \partial_{XX} & 3E_0 \partial_X \end{bmatrix}. \quad (3.4)$$

The harmonic solution of (3.3) is

$$\mathbf{v}_1 = \begin{bmatrix} ae^{i(kX-wT)} + c.c. \\ \phi_0 \end{bmatrix}, \quad (3.5)$$

with k and w as dimensionless wavenumber and frequency of the perturbation, and a and ϕ satisfy the system

$$\begin{bmatrix} i(3E_0k - w) & \frac{E_0k^2}{4} - 3E_0^2k^2 \\ 1 + \frac{k^2(-1+4E_0)}{16E_0} & i(3E_0k - w) \end{bmatrix} \begin{bmatrix} a \\ \phi_0 \end{bmatrix} = \begin{bmatrix} 0 \\ 0 \end{bmatrix}.$$

Therefore, for non-trivial solutions

$$w^2 - 6E_0kw + \frac{E_0k^2}{4} - \frac{k^4}{64} + E_0k^2 \left(6E_0 + \frac{k^2}{4} \right) - \frac{3}{4}E_0^2k^4 = 0. \quad (3.6)$$

The growth rate γ follows from the imaginary part of w as

$$\gamma^2 = -\frac{\Delta_w}{4} = \frac{1}{64} (1 - 12E_0) k^2 [16E_0 - (1 - 4E_0) k^2], \quad (3.7)$$

where Δ_w is the discriminant of (3.6). From (2.4), (3.7) can be written in terms of $\mu = 2\sqrt{E_0}$ as

$$\gamma^2 = \frac{1}{64} (1 - 3\mu^2) k^2 [4\mu^2 - (1 - \mu^2) k^2]. \quad (3.8)$$

Note that γ vanishes at the critical dimensionless wavenumber

$$k_c^2 = \frac{16E_0}{1 - 4E_0} = \frac{4\mu^2}{1 - \mu^2}, \quad (3.9)$$

and the associated frequency $w_c = 3E_0k_c$. It is noted that near the instability threshold k_c , the cDZ equation (2.2) is valid if $k_c^2 < 1$ for allowing Fourier modes of the associated wave surface η with nonnegative wavenumbers only. This yields the upper bound $\mu_m = 0.447$ for μ , nearly the same as the well-known Stokes limiting steepness 0.448. Thus, the above linear analysis is strictly valid for wave steepness $\mu < \mu_m$, largely within the range of validity of the cDZ.

Perturbations with $k < k_c$ are unstable as an indication of subharmonic instability. At the critical steepness $\mu_c = 0.577$ where $E = E_c = 1/12 \approx 0.08$, the perturbation is neutral irrespective of k^\dagger . Despite the fact that this is greater than the Stokes limiting steepness and beyond the validity of the cDZ, the predictions may indicate the correct behavior as pointed out by Crawford *et al.* (1981). At $\mu = \mu_c$, modulational (subharmonic) instability disappears whereas, for $\mu > \mu_c$, superharmonic instability appears. Note that for the

[†] The same threshold holds if non-local effects are retained in the linear stability analysis (Dyachenko & Zakharov (2011)).

Z equation, $\mu_c \approx 0.5\ddagger$ (Crawford *et al.* (1981)). For steep irrotational periodic waves of the Euler equations, superharmonic disturbances are unstable at about $\mu_c \sim 0.41$ (Longuet-Higgins (1978*a*) and Longuet-Higgins & Cokelet (1978)).

In accord with cDZ, from (3.8) the linear growth rate γ of a subharmonic perturbation reduces with respect to the NLS counterpart

$$\gamma_{NLS}^2 = \frac{1}{64}k^2(4\mu^2 - k^2), \quad (3.10)$$

as the steepness μ of the wavetrain increases, especially for small wavenumbers k 's. This is clearly seen in Fig. 3.1, showing the comparison of the theoretical γ and γ_{NLS} against laboratory data for $k = 0.2$ and 0.4 (see also Janssen (1983) and Crawford *et al.* (1981)). This implies that MI is attenuated as μ increases, a well established fact since Lighthill (1965) (see also Longuet-Higgins (1978*b*) and McLean (1982)). This indicates that the likelihood of large breathers reduces as the carrier wave steepness increases, in agreement with the recent experimental results on the Peregrine Breather (PB) presented by Shemer & Alperovich (2013). In particular, for $\mu \sim 0.1$ they observed noticeable deviation from the 1D NLS solution due to significant asymmetric spectral widening. They reported that the “breather does not breathe” since no return to the initial undisturbed wave train is observed. Moreover, the PB amplification is slower and smaller than that predicted by the NLS PB as an indication that MI effects attenuate as waves steepen. This is also confirmed by recent numerical studies of the Euler equations (Slunyaev & Shrira (2013)).

4. Long-time behavior of an unstable wavetrain

We have shown that a finite-amplitude uniform wave train is unstable to infinitesimal perturbations of sufficiently long wavelength, viz. $|k| < k_c$. Near the threshold k_c , the cDZ dynamics of a slightly unstable wavetrain can be determined by means of multiple-scale perturbation methods. Janssen (1981) has already studied the long-time behavior of an unstable wavetrain of the NLS equation. His analysis was restricted to the time domain and revealed that the perturbation evolves periodically in time and exhibits FPU recurrence.

Hereafter, in section 4.1, we extend Janssen's analysis to the cDZ equations (2.9). This will reveal that the perturbation nonlinearly restabilizes as the steepness increases beyond about $\mu_1 \approx 0.27$ whereas Longuet-Higgins (1978*a*) found linear restabilization of a perturbed steep periodic wave at about 0.34. For smaller wave steepness, the perturbation dynamics is of focusing type and dominated by FPU recurrences.

While the cDZ equation is only valid for broadband waves with small steepness, the predictions based on larger values $\mu > \mu_1$ can plausibly be useful in exploring their dynamics near breaking. Indeed, the cDZ may capture new nonlinear features that are not modeled by the 1D NLS and higher-order Dysthe (1979) equations, which do not support finite-time blowup solutions or breaking. Thus, it should be worthwhile to explore the behavior for large values of wave steepness in section 4.2 later on.

4.1. Perturbation dynamics for small μ

Introduce the independent multiple scales $\xi = \epsilon^2 X$, $\tau = \epsilon T$ and consider the ordered expansion for E and ϕ in the small parameter ϵ

\ddagger The two thresholds are slightly different because the cDZ and Z models are given in terms of different canonical variables.

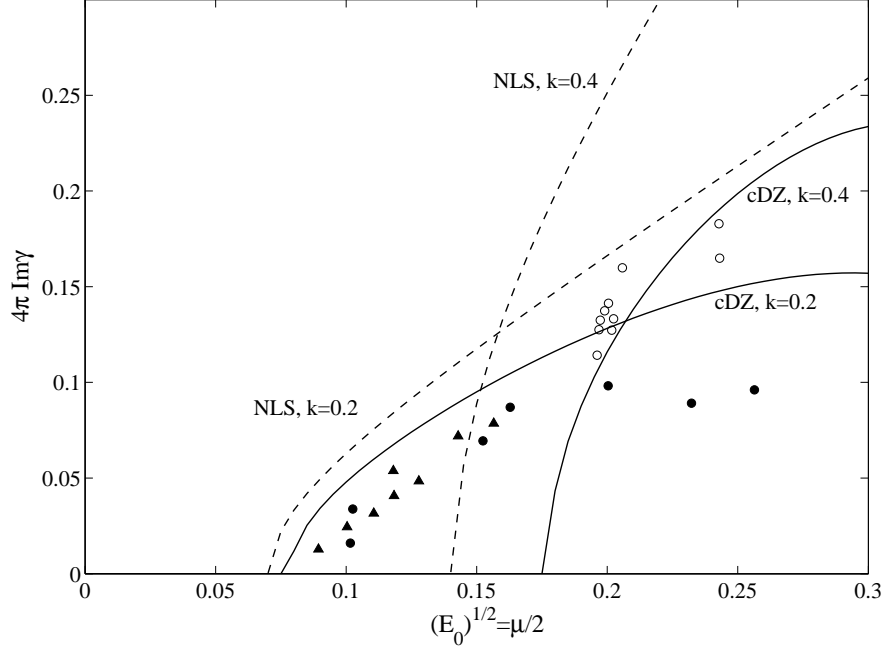


FIGURE 3.1. Linear sideband growth rate $4\pi\text{Im}(\gamma)$ of modulated unstable wave trains as function of the amplitude $\sqrt{E_0} = \mu/2$ for different values of the perturbation wavenumber k : NLS (dashed line) and cDZ (solid line) predictions against data digitized from Fig. 1 in Janssen (1983) (\circ , $k = 0.4$, Lake *et al.* (1977); \bullet , $k = 0.2$, Lake *et al.* (1977); \blacktriangle , $k = 0.2$, Benjamin (1967)).

$$\mathbf{v} = \mathbf{v}_0 + \epsilon \mathbf{v}_1(X, T, \xi, \tau) + \epsilon^2 \mathbf{v}_2(X, T, \xi, \tau) + \epsilon^3 \mathbf{v}_3(X, T, \xi, \tau) + \dots, \quad (4.1)$$

where \mathbf{v}_0 is given in (3.1) and

$$\mathbf{v}_j = \begin{bmatrix} E_j(X, T, \xi, \tau) \\ \phi_j(X, T, \xi, \tau) \end{bmatrix}.$$

The wavenumber k of the perturbation is chosen just below the critical threshold k_c to ensure instability, viz. $k = k_c - \epsilon^2 q_e$, and the arbitrary parameter $q_e > 0$ is of $O(1)$. From (3.7), the corresponding growth rate is of $O(\epsilon)$ and given by

$$\overline{\gamma} = \epsilon \sqrt{\chi q_e}, \quad \chi = E_0 k_c (1 - 12E_0) / 2, \quad (4.2)$$

confirming the well-chosen slow-time scale τ (Janssen (1981)). To $O(\epsilon)$, the asymptotic solution for \mathbf{v} is given by (see Appendix A)

$$\mathbf{v} = \begin{bmatrix} E_0 + \epsilon A(\xi, \tau) e^{i\theta} + c.c. \\ \epsilon \phi_0(\xi, \tau) \end{bmatrix} + O(\epsilon^2),$$

where $\theta = k_c X - w_c T$, the phase is described by

$$\phi_0 = \phi_0(\xi, 0) - \int_0^\tau \frac{k_c^2}{16E_0^2} |A(\xi, s)|^2 ds,$$

and the perturbation amplitude A evolves in accord with the NLS equation

$$i\chi A_\xi = A_{\tau\tau} + \beta|A|^2 A - \chi q_e A, \quad (4.3)$$

where

$$\beta = \frac{2(1-8E_0)(1-56E_0+128E_0^2)}{(1-4E_0)^3} = 2 - 104E_0 + O(E_0^2), \quad (4.4)$$

Note that the linear term in (4.3) could be removed by the canonical transformation $A \rightarrow Ae^{iq_e\xi}$. Since $\mu = 2\sqrt{E_0}$, β and χ can be rewritten as

$$\beta = \frac{2(1-2\mu^2)(1-14\mu^2+8\mu^4)}{(1-\mu^2)^3} = 2 - 26\mu^2 + O(\mu^3), \quad (4.5)$$

and

$$\chi = \frac{\mu^3(1-3\mu^2)}{4\sqrt{1-\mu^2}}. \quad (4.6)$$

The variations of β and χ with μ are shown in Fig. 4.1. Correct to $O(\mu)$, $\beta = 2$ and both the NLS and Dysthe limits of the cDZ lead to the same asymptotic equation. This limit cannot be directly compared to that by Janssen (1981). Indeed, in the latter the long-time evolution is studied near the neutral threshold k_c whereas, in the former the wavenumber k of the perturbation is kept as a free parameter and the NLS dynamics is studied by perturbing the coefficient of the cubic nonlinearities.

The Benjamin-Feir Index (BFI) associated with the NLS equation (4.3) is proportional to the coefficient β of the cubic term. In the focusing regime when $\beta > 0$, the excess kurtosis λ_{40} of a random perturbation is proportional to β^2 (Janssen (2003)). Thus, decreasing values of β imply a smaller λ_{40} and a reduced likelihood of large breathers. When $\beta < 0$, the NLS dynamics is of defocusing type implying suppression of the FPU recurrence ($\lambda_{40} \leq 0$) and the appearance of nonlinear restabilization.

To further study the perturbation dynamics as μ increases from zero, we neglect spatial variability and simplify (4.3) as

$$A_{\tau\tau} + \beta|A|^2 A - \chi q_e A = 0.$$

Following Janssen (1981), this can be interpreted as the equation of motion of a particle in a potential well

$$V(|A|) = -\frac{1}{2}\chi q_e |A|^2 + \frac{1}{4}\beta|A|^4.$$

Evidently, β decreases as μ increases and vanishes at the critical steepness $\mu_1 \approx 0.27$ (see Fig. 4.1). As a result, periodic solutions exist and they are given in terms of Jacobi functions, suggesting FPU recurrence. In this case, the NLS equation (4.3) is of focusing type and the perturbation A evolves to a state of interacting breathers. However, their amplitude and likelihood of occurrence are somewhat diminished because β (and so the BFI) is a decreasing function of μ , which vanishes at μ_1 (see Fig. 4.1). This indicates that homoclinic orbits persist for $\mu \ll \mu_1$ in agreement with the Melnikov analysis applied to a higher-order NLS (HONLS) equation by Schober (2006). This is also confirmed

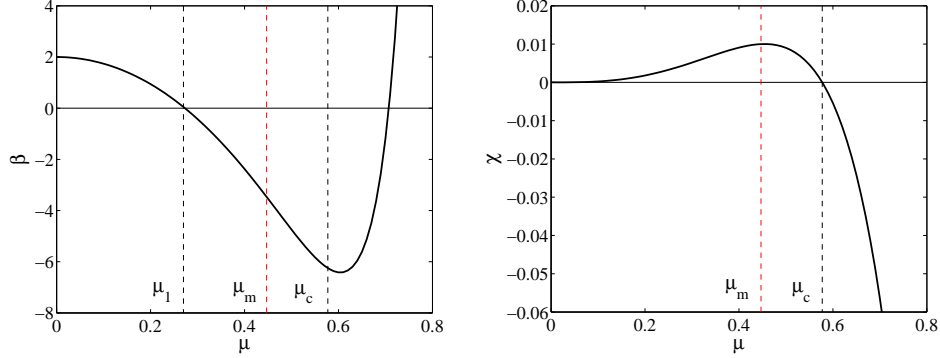


FIGURE 4.1. Coefficients β and χ of the NLS equation (4.3) governing the perturbation to unstable wavetrain as function of wave steepness μ ($\mu_1 \approx 0.27$, $\mu_m \approx 0.447$ and $\mu_c \approx 0.577$). Note that above μ_1 where $\beta < 0$ the perturbation dynamics is of defocusing type.

by the recent experimental observations of higher-order breathers at sufficiently small values ($\sim 0.01 - 0.09$) of wave steepness (Chabchoub *et al.* (2011) and Chabchoub *et al.* (2012)). It is known that observing breathers in experiments where $\mu > 0.1$ is difficult because of wave breaking (Shemer & Alperovich (2013) and Chabchoub *et al.* (2012)). In particular, Slunyaev *et al.* (2013) employ sufficiently small values (≤ 0.1) for μ so as to avoid wave breaking in their numerical simulations of breathers based on the Euler equations.

Finally, where β is positive for $\mu \geq 0.707$, the perturbation dynamics becomes of focusing type again. We have no explanation for this, but it could simply be an artifact of the cDZ equation largely beyond its range of validity.

4.2. An explorative view of dynamics for $\mu > \mu_1$

Despite the fact that the cDZ equation is only valid for broadband waves with small steepness, the predictions beyond $\mu_1 \approx 0.27$ may be still indicative of the trend of wave dynamics. In particular, from Fig. 4.1 β is negative in the range (μ_1, μ_c) and an initially unstable wavetrain restabilizes nonlinearly over the long timescale as an indication that FPU recurrence is suppressed. Indeed, the NLS equation (4.3) is now of defocusing type.

The defocusing character of the long-time perturbation evolution still holds in the range of superharmonic instability ($\mu \geq \mu_c \approx 0.577$, see Fig. 4.1). This may suggest a change in the behavior of the cDZ dynamics as a precursor to steepening of waves and their eventual breaking. In this regard, Bridges (2004) showed that there is very simple mechanism for wave breaking near the change of superharmonic instability. Near the change there is a homoclinic orbit (in time) and so for some initial conditions the solution is attracted to the slow Stokes wave whereas for other wave breaking occurs (Tanaka *et al.* (1987) and Jillians (1989)).

Hereafter, we will explore the long-time evolution of a weak narrowband perturbation to a uniform wavetrain of large amplitude $E_0 > E_c$ or, equivalently large steepness $\mu > \mu_c$. To do so, we consider the conservative form (2.12) of the cDZ equation and apply the multiple-scale perturbation technique in Taniuti & Wei (1968). This will reveal that above E_c , the weakly nonlinear dynamics is of hyperbolic type.

Introduce the slow multiple scales $\xi = \epsilon(X - cT)$, $\tau = \epsilon^2 T$, with c as a wave celerity to be determined and consider the ordered expansion for the local squared envelope amplitude E and wavenumber K in the small parameter ϵ as

$$\mathbf{w} = \mathbf{w}_0 + \epsilon \mathbf{w}_1(\xi, \tau) + \epsilon^2 \mathbf{w}_2(\xi, \tau) + \dots, \quad (4.7)$$

where

$$\mathbf{w}_0 = \begin{bmatrix} E_0 \\ 0 \end{bmatrix}, \quad \mathbf{w}_j = \begin{bmatrix} E_j(\xi, \tau) \\ K_j(\xi, \tau) \end{bmatrix}.$$

For $\mu > \mu_c$, the leading order solution for E and K is given by (see Appendix C)

$$\mathbf{w} = \begin{bmatrix} E_0 \pm \epsilon \frac{\sqrt{-1+3\mu^2}}{2} F(\xi, \tau) \\ \epsilon F(\xi, \tau) \end{bmatrix} + O(\epsilon^2),$$

where $\mu = 2\sqrt{E_0}$, $c = (3\mu \pm \sqrt{-1+3\mu^2})/2$ and F satisfies a non-dispersive Korteweg-de Vries (KdV) equation

$$F_\tau + \beta F F_\xi = 0, \quad (4.8)$$

where

$$\beta = 3 \frac{-6 + 8E_0(9 + E_0) + (-1 + 24E_0)\sqrt{-1 + 12E_0}}{8\sqrt{2}}.$$

Note that celerity c is real for $\mu \geq \mu_c$ or, equivalently $E_0 \geq E_c$, rendering the dynamical equations hyperbolic[†]. This indicates that the wave dynamics is initially non-dispersive and the slope F_ξ blows up in finite time due to steepening. However, (4.8) loses its validity and the weakly nonlinear analysis needs to be extended to higher order. If this is carried out to $O(\epsilon^5)$, it yields

$$F_\tau + \beta F F_\xi + \epsilon (z_1 F_{\xi\xi\xi} + z_2 F^2 F_\xi) + \epsilon^2 z_3 (2F_\xi F_{\xi\xi} + F F_{\xi\xi\xi}) = 0, \quad (4.9)$$

where

$$z_1 = \frac{16E_0(1 - 3E_0) - 1}{64E_0}, \quad z_2 = 3 \frac{-3 + 4E_0(9 + \sqrt{-1 + 12E_0})}{4},$$

and

$$z_3 = (-1 + 12E_0) \frac{8E_0^2 + \sqrt{-1 + 12E_0}}{128\sqrt{2}E_0^2}.$$

This is a modified KdV/Camassa-Holm (CH) equation (Camassa & Holm (1993)), which describes the tendency of a wave perturbation to steepen and break eventually. We point out that, recently, Bridges (2013) has identified a precise mechanism for the appearance of KdV from a NLS equation as that in (4.3) in the defocusing regime. Thus, KdV dynamics is potentially possible in deep water, and further studies along this direction are desirable.

5. Concluding remarks

We have presented the weakly nonlinear dynamics of a perturbation to a linearly unstable wavetrain of the cDZ equation by using multiple-scale perturbation techniques. As wave steepness increases, the analysis predicts that linear growth rate of an unstable

[†] For $\mu < \mu_c$ the analysis is invalid since the system becomes of elliptic types and c is complex.

perturbation and the associated BFI both decrease, thus leading to breather suppression. An analytical solution of the excess kurtosis λ_{40}^{cDZ} of the wave surface described by the cDZ confirms these theoretical results. To $O(\nu^2)$, the excess kurtosis assumes the form (see Appendix D)

$$\lambda_{40}^{cDZ} = \lambda_{40}^{NLS} \left(1 - \frac{4\sqrt{3} + \pi}{8\pi} \nu^2 \right) \approx \lambda_{40}^{NLS} (1 - 0.40\nu^2).$$

This is smaller than the excess kurtosis

$$\lambda_{40}^{NLS} = \frac{\pi}{6\sqrt{3}} \frac{24\mu^2}{\nu^2}$$

associated with the NLS equation, especially as the spectral bandwidth widens and approaches its eventual limit ν (Janssen (2003) and Mori & Janssen (2006)).

Clearly, values of μ greater than μ_1 lie outside the range of relative validity of the cDZ equation. Nonetheless, the predictions indicate that above the critical threshold $\mu_c = 0.577$, subharmonic instability is suppressed, but linearly unstable superharmonic perturbations arise. In comparison, the Z equation yields the same predictions for $\mu > \mu_c = 0.5$. The preceding thresholds are in qualitative agreement with the stability studies of steep periodic waves for which $\mu_c \sim 0.41$ (Longuet-Higgins (1978a) and Longuet-Higgins & Cokelet (1978)).

Above μ_c , the cDZ predicts a perturbation dynamics of defocusing type and FPU recurrence is suppressed. This suggests a change in the behavior of the cDZ dynamics above μ_c as a precursor to wave steepening and eventual breaking, as suggested by Longuet-Higgins (1978a). Indeed, the multiple-scale analysis reveals here that the wave dynamics is of hyperbolic type for $\mu > \mu_c$. Furthermore, the long-time evolution of a weakly nonlinear narrowband perturbation obeys a modified KdV/CH type equation, a model that typically arises in shallow water wave theory. This suggests that there may be physical similarities between shallow- and deep-water waves.

In shallow water of depth h subharmonic instabilities are suppressed at sufficiently small depths and waves of different wavelength tend to travel at the same speed \sqrt{gh} , where g denotes gravitational acceleration. That means that dispersion is suppressed and shorter (longer) waves tend to travel faster (slower) than their linear speeds. Furthermore, local and superharmonic instabilities are enhanced, leading to wave breaking.

In deep water, the cDZ equation predicts that for large steepness $\mu > \mu_c \approx 0.577$, subharmonic disturbances are both linearly and nonlinearly stable, whereas superharmonic instability arises. Moreover, dispersion is also suppressed and shorter waves tend to travel faster than their linear speeds. Indeed, from Eq. (2.10) at the envelope maximum ($E_X = 0$, $E_{XX} < 0$) where a large crest occurs, the local nonlinear frequency

$$\omega_{NL} = \omega_L - \frac{E_{XX}}{4}(1 + K) + E(1 + K)^3 \quad (5.1)$$

increases with respect to the linear counterpart

$$\omega_L = \frac{E_{XX}}{16E} - \frac{K^2}{8} \quad (5.2)$$

as the crest steepens since both E and K increase. As a result, in a reference frame moving with the group velocity of the carrier wave, the local nonlinear phase velocity

$$c_{ph,NL} = \frac{\omega_{NL}}{K} = c_{ph,L} - \frac{E_{XX}}{4K}(1 + K) + E \frac{(1 + K)^3}{K} \quad (5.3)$$

of steepening crests tends to increase with respect to their linear counterpart

$$c_{ph,L} = \frac{\omega_L}{K} = \frac{E_{XX}}{16EK} - \frac{K}{8}. \quad (5.4)$$

A similar trend is also observed for the nonlinear and linear energy flux velocities V_{NL} and V_L beneath a crest. Indeed, from (2.11)

$$V_{NL} = V_L (1 - 12E) + \frac{3}{2}E(1 + K^2) \quad (5.5)$$

and

$$V_L = -\frac{K}{4}. \quad (5.6)$$

As both E and K increase as crests steepen, V_{NL} becomes larger than V_L .

This analysis provides insight into the physics as waves approach conditions conducive to or near maximum recurrence and breaking within the cDZ framework. More explicitly, consider an unsteady slowly varying linear wave group. Wave dispersion induces a generic slowdown of the entire wave structure as each crest in the group reaches its maximum height. In particular, the local phase velocity varies in time and along the group attaining its lowest value $c_{ph,L}$ at the envelope maximum where the largest height of a crest occurs since $E_{XX} < 0$ in (5.4). The crest speed also slows down, and the slowdown is enhanced with increasing spectral bandwidth, resulting in larger crest amplitudes. Indeed, this process causes local energy fluxes beneath the crest to decrease since V_L tends to diminish as crest steepens and K increases [see Eq.(5.6)]. As a result, energy flows from both the upstream and downstream regions of the wave-group maximum, resulting in the growth of crest amplitudes. The stronger the crest deceleration, the larger its amplitude becomes at focus. However, as the crest grows in amplitude, the cDZ equation predicts that nonlinearities counterbalance the linear slowdown, which reduces by wave dispersion suppression, i.e. $c_{ph,NL} > c_{ph,L}$ as seen in Eq. (5.3). Further, in accord with Eq. (5.5), the nonlinear energy flux beneath the crest tends to increase since $V_{NL} > V_L$ limiting potential energy accumulation at the crest.

The preceding physical interpretation of the cDZ predictions on wave groups suggests that dispersion suppression is the leading cause of the observed change in behavior of the cDZ dynamics as wave steepness increases progressively, and it may be the main physical mechanism operative in the neighborhood of maximum recurrence or breaking. This is supported by laboratory studies of unidirectional focusing wave groups by Baldock *et al.* (1996). At focus, they observe an increase in the phases of high-frequency waves relative to their linear counterparts, an indication that wave dispersion is suppressed. More recently, Banner *et al.* (2013) carried out a multifaceted study of steep wave groups by numerical simulations of the Euler equations, laboratory and ocean field experiments. Their results support the preceding cDZ predictions on wave group behavior. In particular, they found that each crest in the group decelerates, linking the slowdown to the reduced initial speed of breaking-wave crests (Rapp & Melville (1990)).

It also appears that directional effects further enhance wave collapse, suppressing the nonlinear focusing induced by modulational instability. In particular, we expect the long-time evolution of a transversely unstable wavetrain of the three-dimensional version of the cDZ equation to obey the two-dimensional hyperbolic NLS equation

$$i\chi A_\xi = A_{\tau\tau} - \delta A_\zeta\zeta + \beta|A|^2A - \chi q_e A, \quad (5.7)$$

where $\zeta = \epsilon Y$ is the slow scale transverse to the main direction of propagation, and δ is a

parameter that depends on steepness and angular spreading. It is well known that (5.7) can support finite-time blow-up solutions depending on the sign of δ (Sulem & Sulem (1999)).

Acknowledgements

FF is grateful to Profs. Michael Banner and M. Aziz Tayfun for useful suggestions during the preparation of the manuscript. FF also thanks Profs. Panayotis Kevrekidis, Taras Lakoba and Jianke Yang for useful discussions on the subject of nonlinear waves and multiple-scale perturbation methods. Financial support is gratefully acknowledged from the National Ocean Partnership Program, through the U.S. Office of Naval Research (Grant BAA 09-012), in partnership with Ifremer.

6. Appendix A: Multiple-scale perturbation analysis near the neutral threshold k_c

Define the slow multiple-scales $\xi = \epsilon^2 X$, $\tau = \epsilon T$, and space and time derivatives are now given by

$$\frac{\partial}{\partial T} = \frac{\partial}{\partial T} + \epsilon \frac{\partial}{\partial \tau}, \quad \frac{\partial}{\partial X} = \frac{\partial}{\partial X} + \epsilon^2 \frac{\partial}{\partial \xi}.$$

Substitution of the ordered expansion (4.1) into the set of the main equations (2.9) yields the following hierarchy of vector equations

$$O(\epsilon) : \quad \partial_T \mathbf{v}_1 + \mathcal{M}_0 \mathbf{v}_1 = 0 \quad (6.1)$$

$$O(\epsilon^2) : \quad \partial_T \mathbf{v}_2 + \mathcal{M}_0 \mathbf{v}_2 = -\partial_\tau \mathbf{v}_1 + \mathbf{R}_2(\mathbf{v}_1), \quad (6.2)$$

$$O(\epsilon^3) : \quad \partial_T \mathbf{v}_3 + \mathcal{M}_0 \mathbf{v}_3 = -\partial_\tau \mathbf{v}_2 - \partial_{\tau\tau} \mathbf{v}_1 - \mathcal{M}_3 \mathbf{v}_1 + \mathbf{R}_3(\mathbf{v}_1, \mathbf{v}_2) \quad (6.3)$$

where the linear differential matrix operator

$$\mathcal{M}_3 = \begin{bmatrix} 3E_0 \partial_\xi & -\frac{E_0(1-12E_0)}{4} \partial_{X\xi} \\ \frac{1-4E_0}{16E_0} \partial_{X\xi} & 3E_0 \partial_\xi \end{bmatrix}$$

and \mathcal{M}_0 follows from (3.4). The source terms \mathbf{R}_2 and \mathbf{R}_3 are given in Appendix B. In particular, \mathbf{R}_2 is a quadratic polynomial of the components of \mathbf{v}_1 , viz. E_1 and ϕ_1 and their space derivatives whereas, \mathbf{R}_3 is a cubic polynomial of the components of both \mathbf{v}_1 and \mathbf{v}_2 and their space derivatives. Hereafter, the hierarchy (6.1-6.3) is solved order by order by removing the secularities that are condition on the nonlinear source terms. This is equivalent to imposing the orthogonality of the right-hand sides of (6.2) and (6.3) to the null-space of the adjoint operator \mathcal{M}_0^* .

To $O(\epsilon)$, (6.1) is linear and the its general solution is given by

$$\mathbf{v}_1 = \begin{bmatrix} Ae^{i(kX-wT)} + c.c. \\ \phi_0 \end{bmatrix},$$

where the unknown coefficients A and ϕ_0 are function of the slow scales ξ and τ . Near

the linear instability threshold, $k = k_c - q_e \epsilon^2$ with $q_e > 0$, and \mathbf{v}_1 is re-written as

$$\mathbf{v}_1 = \begin{bmatrix} a(\xi, \tau) e^{i\theta} + c.c. \\ \phi_0(\xi, \tau) \end{bmatrix}, \quad (6.4)$$

where $\theta = k_c X - w_c T$, and the auxiliary amplitude

$$a(\xi, \tau) = A(\xi, \tau) e^{-iq_e \xi}. \quad (6.5)$$

To $O(\epsilon^2)$, \mathbf{v}_2 of (6.2) is given by the sum of particular solution $\mathbf{v}_{2,p}$ and the homogenous solution $\mathbf{v}_{2,h}$ as

$$\mathbf{v}_2 = \mathbf{v}_{2,p} + \mathbf{v}_{2,h}, \quad (6.6)$$

where

$$\mathbf{v}_{2,p} = \begin{bmatrix} q_0 + q_{12} e^{2i\theta} + c.c. \\ q_{21} e^{i\theta} + q_{22} e^{2i\theta} + c.c. \end{bmatrix}, \quad \mathbf{v}_{2,h} = \begin{bmatrix} \alpha_1 e^{i\theta} + c.c. \\ \alpha_3 \end{bmatrix}, \quad (6.7)$$

Here, the unknown coefficients $q_0, q_{12}, q_{21}, q_{22}, \alpha_1$ and α_3 are function of the slow scales. Using MATHEMATICA 8.0 (2010) coupled with cumbersome algebra shows that the righthand side of (6.2) contains secular terms. Indeed,

$$\mathbf{S}_2 = \begin{bmatrix} \frac{1}{4} e^{i\theta} [4\partial_\tau a + E_0 (1 - 12E_0) k_c^2 q_{21}] + c.c. \\ \left(\partial_\tau \phi_0 + \frac{k_c^2}{16E_0^2} |a|^2 a + q_0 \right) \end{bmatrix} + \mathbf{T},$$

and \mathbf{T} contains the non-secular higher-order harmonics contributions. The secular terms can be removed if q_{21} and q_0 are chosen such as

$$q_0 = -\phi_{0\tau} - \frac{k_c^2}{16E_0^2} |a|^2, \quad q_{21} = -\frac{4a_\tau}{E_0 (1 - 12E_0) k_c^2}. \quad (6.8)$$

One can now solve for the non-secular source terms and obtain the other two coefficients as

$$q_{12} = -\frac{3a^2 k_c}{8E_0 [4E_0 - k_c^2 (1 - 4E_c)]}, \quad q_{22} = -ia^2 \varepsilon \frac{12 - k_c^2}{4E_0 (1 - 12E_0) k_c}. \quad (6.9)$$

The coefficients (α_1, α_3) of the homogenous part together with the amplitude a can be solved at the next order as follows. To $O(\epsilon^3)$, substituting the solutions for v_1 and v_2 (Eqs. 6.4, 6.6, 6.8, 6.9) into the right-hand side of (6.3) yields a source term that still contains secular terms given by

$$\mathbf{S}_3 = \begin{bmatrix} S_{10} + S_{11} e^{i\theta} + c.c. \\ S_{20} + S_{21} e^{i\theta} + c.c. \end{bmatrix},$$

where

$$S_{10} = q_{0\tau}, \quad (6.10)$$

$$S_{11} = \alpha_{1\tau} + 3E_0 a_\xi - 3ik_c a \phi_{0\tau} + d|a|^2 a, \quad (6.11)$$

$$S_{20} = \alpha_{3\tau} + 3E_0\phi_{0\xi} - 3ik_c \frac{1 - 4E_0}{4E_0^2(1 - 12E_0)} (a^* a_\tau - aa_\tau^*), \quad (6.12)$$

$$S_{21} = q_{21\tau} - \frac{k^2}{16E_0^2} a\phi_{0\tau} + ik \frac{1 - 4\epsilon^2 E_0}{8E_0} a_\xi + d_2 |a|^2 a, \quad (6.13)$$

and

$$d = ik \frac{-48E_0(1 - 12E_0) + k_c^2(-3 + 108E_0 + 64E_0^2(-13 + 24E_0))}{32E_0^2(1 - 16E_0 + 48E_0^2)},$$

$$d_2 = -\frac{3 - 88E_0 + 576E_0^2 - 1024E_0^3}{2E_0^2(1 - 12E_0)(1 - 4E_0)^2}.$$

To have bounded solutions for \mathbf{v}_3 , these secular terms must be removed. From (6.10), $S_{10} = 0$ yields $q_0 = c_0$, where the constant c_0 can be set equal to zero, if at initial time $q_0(\tau = 0) = 0$. From (6.8), it then follows that

$$\phi_{0\tau} = -\frac{k_c^2}{16E_0^2} |a|^2.$$

Imposing $S_{11} = 0$ and $S_{12} = 0$ yield two equations from which one can solve for α_1 and α_3 once a is known. The evolution equation for a follows from (6.13) by setting $S_{21} = 0$, which yields

$$i\chi a_\xi - a_{\tau\tau} - \beta |a|^2 a = 0, \quad (6.14)$$

where χ is given in (3.7) and

$$\beta = \frac{2(1 - 8E_0)(1 - 56E_0 + 128E_0^2)}{(1 - 4E_0)^3}$$

The main equation (4.3) for A follows from (6.14) by substituting $a = Ae^{-iq_e\xi}$ [see Eq. (6.5)] and the derivative $a_\xi = (A_\xi - iq_e) e^{-iq_e\xi}$.

Appendix B: Source terms

The components of

$$\mathbf{R}_2 = \begin{bmatrix} R_{21} \\ R_{22} \end{bmatrix}$$

are given by

$$\begin{aligned} R_{21} = & 3E_1 E_{1X} + \frac{1}{4}(-1 + 24E_0)(E_1 \phi_{1XX} + E_{1X} \phi_{1X}) + \\ & + \frac{1}{4} E_{1X} (E_{1XX} + E_0^2 \phi_{1X} \phi_{1XX}), \end{aligned}$$

and

$$\begin{aligned} R_{22} = & \frac{1}{32E_0^2} [-E_{1X}^2 + E_1(-2E_{1XX} + 96E_0^2 \phi_{1X}) + \\ & 4E_0^2(-1 + 24E_0) \phi_{1X}^2 - 8E_0^2(\phi_{1X}^2 E_{1XX} + E_{1X} \phi_{1XX})], \end{aligned}$$

and those of

$$\mathbf{R}_3 = \begin{bmatrix} R_{31} \\ R_{32} \end{bmatrix}$$

by

$$\begin{aligned} R_{31} = & \frac{1}{4} (E_{2X} E_{1XX} + E_{1X} E_{2XX}) + \frac{1}{4} (-1 + 24E_0) (\phi_{1X} E_{2X} + E_2 \phi_{1XX} + E_1 \phi_{2XX}) + \\ & 3 (E_1^2 \phi_{1XX} + 2E_1 E_{1X} \phi_{1X} + 2E_0 E_{1X} \phi_{2X}) + \\ & 3 (E_0^2 \phi_{2X} \phi_{1XX} + E_0^2 \phi_{1X} \phi_{2XX} + E_1 E_0 \phi_{1X} \phi_{1XX} + E_0 E_{1X} \phi_{1X}^2) + \\ & + 3 (E_1 E_{2X} + E_2 E_{1X}) - \frac{1}{4} E_{1X} \phi_{2X}, \end{aligned}$$

and

$$\begin{aligned} R_{33} = & \frac{1}{16E_0^3} [E_1 E_{1X}^2 + E_1^2 E_{1XX} - E_0 (E_2 E_{1XX} + E_{1X} E_{2X} + E_1 E_{2XX})] - \frac{\phi_{1X} \phi_{2X}}{4} + \\ & 3 (E_2 \phi_{1X} + E_1 \phi_{2X}) + 3 (E_1 \phi_{1X}^2 + 2E_0 \phi_{1X} \phi_{2X}) + \\ & + \frac{1}{4} (E_0 \phi_{1X}^3 - E_{2XX} \phi_{1X} - E_{2X} \phi_{1XX} - E_{1XX} \phi_{2X} - E_{1X} \phi_{2XX}). \end{aligned}$$

7. Appendix C: Multiple-scale perturbation analysis for $\mu > \mu_c$

We draw on Taniuti & Wei (1968) and define the multiple scales $\xi = \epsilon(X - cT)$, $\tau = \epsilon^2 T$, with c as a wave celerity to be determined. Substitution of the ordered expansion (4.7) into the set of the main equations (2.12) for E and K yields the following hierarchy of vector equations

$$O(\epsilon^2): \quad (-c\mathbf{I} + \mathbf{V})\partial_\xi \mathbf{w}_1 = 0 \quad (7.1)$$

$$O(\epsilon^3): \quad (-c\mathbf{I} + \mathbf{V})\partial_\xi \mathbf{w}_2 = -\partial_\tau \mathbf{w}_1 + \mathbf{R}(\mathbf{w}_1), \quad (7.2)$$

where

$$\mathbf{V} = \begin{bmatrix} 3E_0 & -\frac{E_0(1-12E_0)}{4} \\ 1 & 3E_0 \end{bmatrix} \quad (7.3)$$

and the source term

$$\mathbf{R} = - \begin{bmatrix} 3K_1 K_{1\xi} + \frac{-1+24E_0}{4} K_1 E_{1\xi} \\ 3(K E_{1\xi} + E_1 K_{1\xi}) + \frac{-1+24E_0}{4} K_1 K_{1\xi} \end{bmatrix}$$

The eigenvalues of \mathbf{V} follows as

$$\lambda_{1,2} = 3E_0 \pm \frac{1}{2} \sqrt{-1 + 12E_0}.$$

and the associated right- and left- eigenvectors are given, respectively, by

$$\mathbf{q}_{1,2} = \begin{bmatrix} \pm \frac{\sqrt{-1+12E_0}}{2} \\ 1 \end{bmatrix}, \quad \mathbf{p}_{1,2} = \begin{bmatrix} \pm \frac{2}{\sqrt{-1+12E_0}} & 1 \end{bmatrix}.$$

The eigenvalues are real for $E_0 \geq E_c$ denoting the hyperbolic nature of hierarchy equations; however \mathbf{V} is diagonalizable only for $E_0 > E_c$ (For $E_0 = E_c$, \mathbf{V} can be made triangular via the Jordan decomposition, but this case will not be considered here). As a result, to $O(\epsilon^2)$ we set $c = \lambda_j$ and the solution of (7.1) is given by

$$\mathbf{w}_1 = \mathbf{q}_j F(\xi, \tau), \quad (7.4)$$

and F is solved to the next order. Indeed, to $O(\epsilon^3)$ the compatibility condition for (7.2) imposes its source term to be orthogonal to the corresponding row left-eigenvector \mathbf{p}_j of \mathbf{V} (see Taniuti & Wei (1968)). This yields

$$F_\tau - \frac{\mathbf{p}_j R(\mathbf{q}_j F)}{\mathbf{p}_j \mathbf{q}_j} = 0,$$

which after some simplifications yields the non-dispersive KdV equation (4.8).

8. Appendix D: Excess kurtosis

Drawing upon Mori & Janssen (2006), the excess kurtosis of weakly nonlinear waves that obey the local cDZ equation is given by

$$\lambda_{40}(t) = \frac{24\mu^2}{\nu^2} \iiint T_{123} \sqrt{\frac{w}{w_1 w_2 w_3}} S_1 S_2 S_3 \frac{1 - \cos(\Delta \omega_0 t)}{\Delta} dk_1 dk_2 dk_3, \quad (8.1)$$

where the dimensionless frequency $w_j = \sqrt{k_j}$, $\Delta = w + w_1 - w_2 - w_3$, the dimensionless Gaussian spectra

$$S_j(k_j) = \frac{1}{\sqrt{2\pi}} e^{-\frac{(k_j-1)^2}{2\nu^2}},$$

and the kernel T_{123} is given in Dyachenko & Zakharov (2011) as

$$T_{123} = \frac{1}{8\pi} [k k_1 (k + k_1) + k_2 k_3 (k_2 + k_3)].$$

To solve for (8.1), define the auxiliary variables $z_j = (k_j - 1)/\nu$. Then, correct to $O(\nu^2)$, Eq. (8.1) reduces to

$$\lambda_{40} = \frac{24\mu^2}{\nu^2} \iiint \frac{e^{-\frac{z_1^2 + z_2^2 + z_3^2}{2\nu^2}}}{(2\pi)^{3/2}} G \frac{1 - \cos(Z\alpha)}{Z/4} dz_1 dz_2 dz_3, \quad (8.2)$$

where $\alpha = \frac{1}{4}\nu^2\omega_0 t$, $Z = -(z_1 - z_2)(z_1 - z_3)$, and

$$G = 1 + \frac{\nu}{2} (-z_1 + 3z_2 + 3z_3) + \frac{\nu^2}{8} (-3z_1^2 + 4z_2^2 + 10z_2 z_3 + 4z_3^2).$$

Following Fedele *et al.* (2010),

$$\frac{d\lambda_{40}}{d\alpha} = \frac{24\mu^2}{\nu^2} \iiint \frac{e^{-\frac{z_1^2 + z_2^2 + z_3^2}{2\nu^2}}}{(2\pi)^{3/2}} G \sin(Z\alpha) dz_1 dz_2 dz_3,$$

and in vector notation

$$\frac{d\lambda_{40}}{d\alpha} = \frac{24\mu^2}{\nu^2} \Im [J(\alpha)], \quad (8.3)$$

where $\Im(x)$ denotes the imaginary part of x ,

$$J(\alpha) = \iiint \frac{e^{-\frac{1}{2}\mathbf{z}^T \boldsymbol{\Omega} \mathbf{z}}}{(2\pi)^{3/2}} \left(1 + \frac{\nu}{2} \mathbf{c}^T \mathbf{z} + \frac{\nu^2}{8} \mathbf{z}^T \mathbf{A} \mathbf{z} \right) d\mathbf{z}, \quad (8.4)$$

and

$$\mathbf{z} = \begin{bmatrix} z_1 \\ z_2 \\ z_3 \end{bmatrix}, \quad \mathbf{c} = \begin{bmatrix} -1 \\ 3 \\ 3 \end{bmatrix},$$

$$\boldsymbol{\Omega} = \begin{bmatrix} 1+2i\alpha & -i\alpha & -i\alpha \\ -i\alpha & 1 & i\alpha \\ -i\alpha & i\alpha & 1 \end{bmatrix}, \quad \mathbf{A} = \begin{bmatrix} -3 & 0 & 0 \\ 0 & 4 & 5 \\ 0 & 5 & 4 \end{bmatrix},$$

The Gaussian integral (8.4) can be solved exactly by the change of variable $\mathbf{s} = \mathbf{Q}^{-1}\mathbf{z}$, where \mathbf{Q} is the eigenvector matrix of $\boldsymbol{\Omega} = \mathbf{Q}^{-1}\mathbf{D}\mathbf{Q}$, and \mathbf{D} that of the eigenvalues. Then,

$$J(\alpha) = \iiint \frac{e^{-\frac{1}{2}\mathbf{s}^T \mathbf{D} \mathbf{s}}}{(2\pi)^{3/2}} \left(1 + \frac{\nu^2}{8} \mathbf{s}^T \mathbf{Q}^{-T} \mathbf{A} \mathbf{Q}^{-1} \mathbf{s} \right) d\mathbf{s},$$

and after integration

$$J(\alpha) = \frac{24 + 48i\alpha + 72\alpha^2 + \nu^2 (5 + 10i\alpha - 9\alpha^2)}{24 (1 + 2i\alpha + 3\alpha^2)^{3/2}}.$$

Integrating (8.3) in α with $J(0) = 0$ yields

$$\lambda_{40}^{cDZ} = \frac{24\mu^2}{\nu^2} \left[\left(\frac{\pi}{6\sqrt{3}} - \nu^2 \frac{12 + \pi\sqrt{3}}{144} \right) - \Im \left(\frac{2\nu^2 (5\alpha - i) + i\sqrt{3} (8 - \nu^2) \sqrt{1 + 2i\alpha + 9\alpha^2} \arcsin \left(\frac{1-3i\alpha}{2} \right)}{\sqrt{1 + 2i\alpha + 3\alpha^2}} \right) \right].$$

At steady state, as $\alpha \rightarrow \infty$,

$$\lambda_{40}^{cDZ} = \frac{24\mu^2}{\nu^2} \left(\frac{\pi}{6\sqrt{3}} - \nu^2 \frac{12 + \pi\sqrt{3}}{144} \right).$$

The NLS limit derived by Mori & Janssen (2006) follows by neglecting $O(\nu^2)$ terms within parenthesis, namely

$$\lambda_{40}^{NLS} = \frac{\pi}{6\sqrt{3}} \frac{24\mu^2}{\nu^2}.$$

Thus, correct to $O(\nu^2)$,

$$\lambda_{40}^{cDZ} = \lambda_{40}^{NLS} \left(1 - \frac{4\sqrt{3} + \pi}{8\pi} \nu^2 \right) \approx \lambda_{40}^{NLS} (1 - 0.40\nu^2).$$

REFERENCES

- 8.0, MATHEMATICA 2010 Wolfram research, inc. .
- ABLOWITZ, M. J. & SEGUR, H. 1981 *Solitons and the Inverse Scattering Transform*. Society for Industrial & Applied Mathematics.
- BALDOCK, T. E., SWAN, C. & TAYLOR, P. H. 1996 A laboratory study of nonlinear surface waves on water. *Philosophical Transactions of the Royal Society of London. Series A: Mathematical, Physical and Engineering Sciences* **354** (1707), 649–676.
- BANNER, M. L., BARTHELEMY, X., FEDELE, F., ALLIS, M., BENETAZZO, A., DIAS, F. & PEIRSON, W.L. 2013 Unexpected wave group behaviour challenges use of stokes theory for ocean waves (<http://arxiv.org/abs/1305.3980>).
- BENJAMIN, T. B. 1967 Instability of periodic wavetrains in nonlinear dispersive systems. *Proc. R. Soc. London, Ser. A* **299**(59).
- BENJAMIN, T. B. & FEIR, J. E. 1967 The disintegration of wavetrains in deep water. Part 1. *J. Fluid Mech.* **27** (417).
- BRIDGES, THOMAS J. 2004 Superharmonic instability, homoclinic torus bifurcation and water-wave breaking. *Journal of Fluid Mechanics* **505**, 153–162.
- BRIDGES, THOMAS J. 2013 A universal form for the emergence of the korteweg–de vries equation. *Proceedings of the Royal Society A: Mathematical, Physical and Engineering Science* **469** (2153).
- CAMASSA, R. & HOLM, D. 1993 An integrable shallow water equation with peaked solitons. *Phys. Rev. Lett.* **71**(11), 1661–1664.
- CHABCHOUB, A., HOFFMANN, N., ONORATO, M. & AKHMEDIEV, N. 2012 Super rogue waves: Observation of a higher-order breather in water waves. *Phys. Rev. X* **2**, 011015.
- CHABCHOUB, A., HOFFMANN, N. P. & AKHMEDIEV, N. 2011 Rogue wave observation in a water wave tank. *Phys. Rev. Lett.* **106**, 204502.
- CHU, V. H. & MEI, C. C. 1970 On slowly-varying Stokes waves. *Journal of Fluid Mechanics* **41**, 873–887.
- CLAMOND, D., FRANCIUS, M., GRUE, J. & KHARIF, C. 2006 Long time interaction of envelope solitons and freak wave formations. *Eur. J. Mech. B/Fluids* **25** (5), 536–553.
- CRAWFORD, DONALD R., LAKE, BRUCE M., SAFFMAN, PHILIP G. & YUEN, HENRY C. 1981 Stability of weakly nonlinear deep-water waves in two and three dimensions. *Journal of Fluid Mechanics* **105**, 177–191.
- DYACHENKO, A. I. & ZAKHAROV, V. E. 2011 Compact Equation for Gravity Waves on Deep Water. *JETP Lett.* **93** (12), 701–705.
- DYACHENKO, A. I., KACHULIN D. I. & ZAKHAROV, V. E. 2013 On the nonintegrability of the free surface hydrodynamics. *JETP Lett.* **98** (1), 48–52.
- DYSTHE, K. B. 1979 Note on a modification to the nonlinear Schrödinger equation for application to deep water. *Proc. R. Soc. Lond. A* **369**, 105–114.
- DYSTHE, K. B. & TRULSEN, K. 1999 Note on breather type solutions of the NLS as models for freak-waves. *Physica Scripta* **T82**, 48–52.
- DYSTHE, K. B., KROGSTAD H. E. & MULLER, P. 2008 Oceanic rogue waves. *Annual Review of Fluid Mechanics* **40**, 287–310.
- FEDELE, F., CHERNEVA, Z., TAYFUN, M. A. & SOARES, C. GUEDES 2010 Nonlinear schrodinger invariants and wave statistics. *Physics of Fluids* **22** (3), 036601.
- FEDELE, F. & DUTYKH, D. 2012 Special solutions to a compact equation for deep-water gravity waves. *Journal of Fluid Mechanics* **712**, 646–660.
- FERMI, E., PASTA J. ULAM H.C. 1955 Studies of non linear problems. *Tech. Rep.* Report No. LA-1940. Los Alamos Scientific Laboratory.
- GRAMSTAD, O. & TRULSEN, K. 2007 Influence of crest and group length on the occurrence of freak waves. *Journal of Fluid Mechanics* **582**, 463–472.
- HENDERSON, K.L., PEREGRINE, D.H. & DOLD, J.W. 1999 Unsteady water wave modulations: fully nonlinear solutions and comparison with the nonlinear schrödinger equation. *Wave Motion* **29** (4), 341 – 361.
- JANSSEN, P.A.E.M. 1981 Modulational instability and the fermi-pasta-ulam recurrence. *Physics of Fluids* **24**, 23–26.
- JANSSEN, P.A.E.M. 1983 On a fourth-order envelope equation for deep-water waves. *J. Fluid Mech* **126**, 1–11.

- JANSSEN, PETER A. E. M. 2003 Nonlinear four-wave interactions and freak waves. *Journal of Physical Oceanography* **33** (4), 863–884.
- JILLIANS, W. J. 1989 The superharmonic instability of stokes waves in deep water. *Journal of Fluid Mechanics* **204**, 563–579.
- KHARIF, C. & PELINOVSKY, E. 2003 Physical mechanisms of the rogue wave phenomenon. *Eur. J. Mech. B/Fluids* **22**, 603–634.
- KHARIF, C., PELINOVSKY, E. & SLUNYAEV, A. 2009 *Rogue Waves in the Ocean*. Springer.
- KRASITSKII, V. P. 1994 On reduced equations in the Hamiltonian theory of weakly nonlinear surface waves. *J. Fluid Mech* **272**, 1–20.
- LAKE, BRUCE M., YUEN, HENRY C., RUNGALDIER, HARALD & FERGUSON, WARREN E. 1977 Nonlinear deep-water waves: theory and experiment. part 2. evolution of a continuous wave train. *Journal of Fluid Mechanics* **83**, 49–74.
- LIGHTHILL, M. J. 1965 Contributions to the theory of waves in non-linear dispersive systems. *IMA Journal of Applied Mathematics* **1** (3), 269–306.
- LONGUET-HIGGINS, M. S. 1978*a* The instabilities of gravity waves of finite amplitude in deep water. i. superharmonics. *Proceedings of the Royal Society of London. A. Mathematical and Physical Sciences* **360** (1703), 471–488.
- LONGUET-HIGGINS, M. S. 1978*b* The instabilities of gravity waves of finite amplitude in deep water ii. subharmonics. *Proceedings of the Royal Society of London. A. Mathematical and Physical Sciences* **360** (1703), 489–505.
- LONGUET-HIGGINS, M. S. & COKELET, E. D. 1978 The deformation of steep surface waves on water. ii. growth of normal-mode instabilities. *Proceedings of the Royal Society of London. A. Mathematical and Physical Sciences* **364** (1716), 1–28.
- MCLEAN, JOHN W. 1982 Instabilities of finite-amplitude water waves. *Journal of Fluid Mechanics* **114**, 315–330.
- MORI, NOBUHITO & JANSSEN, PETER A. E. M. 2006 On kurtosis and occurrence probability of freak waves. *Journal of Physical Oceanography* **36** (7), 1471–1483.
- OSBORNE, A. 2010 *Nonlinear ocean waves and the inverse scattering transform*, , vol. 97. Elsevier.
- OSBORNE, A. R., ONORATO, M. & SERIO, M. 2000 The nonlinear dynamics of rogue waves and holes in deep-water gravity wave trains. *Phys. Lett. A* **275** (5-6), 386–393.
- PEREGRINE, D. H. 1983 Water waves, nonlinear Schrödinger equations and their solutions. *Journal of the Australian Mathematical Society Series B* **25**, 16–43.
- RAPP, R. J. & MELVILLE, W. K. 1990 Laboratory measurements of deep-water breaking waves. *Philosophical Transactions of the Royal Society of London. Series A, Mathematical and Physical Sciences* **331** (1622), 735–800.
- SCHÖBER, C.M. 2006 Melnikov analysis and inverse spectral analysis of rogue waves in deep water. *European Journal of Mechanics - B/Fluids* **25** (5), 602 – 620.
- SHEMER, L. & ALPEROVICH, S.H. 2013 Peregrine breather revisited. *Physics of Fluids* **25**, 051701.
- SLUNYAEV, A., PELINOVSKY, E., SERGEEVA, A., CHABCHOUB, A., HOFFMANN, N., ONORATO, M. & AKHMEDIEV, N. 2013 Super-rogue waves in simulations based on weakly nonlinear and fully nonlinear hydrodynamic equations. *Phys. Rev. E* **88**, 012909.
- SLUNYAEV, ALEXEY V. & SHRIRA, VICTOR I. 2013 On the highest non-breaking wave in a group: fully nonlinear water wave breathers versus weakly nonlinear theory. *Journal of Fluid Mechanics* **735**, 203–248.
- SULEM, C. & SULEM, P.-L. 1999 *The Nonlinear Schrödinger Equation. Self-Focusing and Wave Collapse*. Springer-Verlag, New York.
- TANAKA, MITSUHIRO 1990 Maximum amplitude of modulated wavetrain. *Wave Motion* **12** (6), 559 – 568.
- TANAKA, M., DOLD, J. W., LEWY, M. & PEREGRINE, D. H. 1987 Instability and breaking of a solitary wave. *Journal of Fluid Mechanics* **185**, 235–248.
- TANIUTI, TOSIYA & WEI, CHAU-CHIN 1968 Reductive perturbation method in nonlinear wave propagation. i. *Journal of the Physical Society of Japan* **24** (4), 941–946.
- YANG, J. 2010 *Nonlinear Waves in Integrable and Nonintegrable Systems*. SIAM.
- ZAKHAROV, V. E. 1999 Statistical theory of gravity and capillary waves on the surface of a finite-depth fluid. *Eur. J. Mech. B/Fluids* **18** (3), 327–344.

- ZAKHAROV, V. E. & SHABAT, A. B. 1972 Exact Theory of Two-dimensional Self-focusing and One-dimensional Self-modulation of Waves in Nonlinear Media. *Soviet Physics-JETP* **34**, 62–69.